coatings

MDPI

Article

Effects of Surface Finishing Protocols and Simulated Toothbrushing on Three-Dimensional Surface Topography and Wettability of Feldspathic CAD/CAM Ceramics

Zeynep Yeşil [1,2], Zahide Aydın [3,*] and Firas Süleymanoğlu [4]

[1] Department of Prosthodontics, Faculty of Dentistry, Atatürk University, 25240 Erzurum, Türkiye; zyesilz@hotmail.com
[2] Department of Prosthodontics, Faculty of Dentistry, Erzincan Binali Yıldırım University, 24100 Erzincan, Türkiye
[3] Erzurum Oral and Dental Health Center, Ministry of Health, 25050 Erzurum, Türkiye
[4] Department of Prosthodontics, Faculty of Dentistry, University of Health Sciences, 34668 Istanbul, Türkiye; firas.suleymanoglu@sbu.edu.tr
* Correspondence: dt.zahideaydin@gmail.com; Tel.: +90-501-036-2528

Highlights

What are the main findings?

- The three-step OptraFine polishing protocol yielded the lowest Sa and remained smoother than the glazed surfaces after brushing.
- Simulated toothbrushing corresponding to 2 years increased Sz, Sku, and Sdr, indicating localized defect formation rather than uniform wear.
- Toothbrushing decreased the water contact angle in all finishing groups except the glaze-only group.

What are the implications of the main findings?

- Complete three-step OptraFine polishing may serve as an alternative to reglazing in terms of surface roughness.
- Polishing before glazing did not reduce Sa but resulted in the lowest Sku and contact angle values.
- Polishing outcomes are system-specific; results obtained with one diamond polishing system cannot be extrapolated to others.
- Combining areal 3D parameters with wettability measurements reveals brushing-induced changes that mean roughness alone may not detect.

Abstract

Surface finishing governs the surface integrity of feldspathic CAD/CAM ceramics; however, the stability of finished surfaces under toothbrushing remains unclear. This in vitro study evaluated the effects of four finishing protocols (OptraFine polishing, EVE polishing, glazing, and OptraFine polishing followed by glazing) and simulated toothbrushing on the three-dimensional surface topography and wettability of this ceramic. Forty-eight disc-shaped specimens ($n = 12$) were analyzed before and after 20,000 brushing cycles (approximately 2 years of clinical use) using the ISO 25178 areal parameters Sa, Sz, Ssk, Sku, and Sdr and the static water contact angle, complemented by scanning electron microscopy and energy-dispersive X-ray spectroscopy (EDS). Data were analyzed using generalized estimating equations. The finishing protocol significantly affected all evaluated parameters. Toothbrushing increased Sz, Sku, and Sdr overall and significantly decreased the contact angle in all groups except the Glaze group, whereas its effect on Sa was protocol-dependent, with significant increases only in the OptraFine and OptraFine + Glaze groups. OptraFine

Check for updates

Academic Editor: Seunghan Oh

Received: 29 October 2026
Revised: 13 November 2026
Accepted: 16 November 2026
Published: 18 November 2026

Copyright: © 2026 by the authors. Licensee MDPI, Basel, Switzerland. This article is an open access article distributed under the terms and conditions of the Creative Commons Attribution (CC BY) license.

produced the lowest Sa and remained smoother than both glazed groups after brushing. EDS suggested a compositional shift in the glazed surfaces toward that of the ceramic substrate. The complete three-step OptraFine sequence may serve as an alternative to reglazing in terms of surface roughness, whereas polishing before glazing did not reduce Sa.

Keywords: dental porcelain; CAD/CAM; surface properties; wettability; toothbrushing

1. Introduction

CAD/CAM technologies have significantly transformed restorative dentistry by enabling the standardized, efficient, and precise fabrication of dental restorations [1]. The long-term clinical performance of CAD/CAM ceramic restorations, however, depends largely on the preservation of surface integrity. Surface characteristics, particularly roughness and wettability, influence the biological and esthetic performance of restorations and may be altered by routine oral hygiene procedures [2]. Among the available CAD/CAM materials, feldspathic ceramics remain widely used because of their excellent translucency and esthetic properties [3]. However, their predominantly glassy matrix renders them more susceptible to surface degradation and mechanical complications, making them a suitable model material for investigating the effects of finishing procedures and aging [4].

The clinical performance of feldspathic CAD/CAM ceramics is closely related to surface roughness and wettability, which influence biological interactions and adhesive performance [5]. Increased surface roughness promotes bacterial adhesion, biofilm accumulation, and antagonist wear [6,7]. Although a roughness threshold of approximately 0.2 μm (Ra) has been associated with increased plaque accumulation [8,9], this threshold cannot be directly extrapolated to three-dimensional parameters such as Sa [10]. Wettability, commonly characterized by the contact angle and surface free energy, influences salivary protein adsorption and acquired pellicle formation [11,12] and is itself affected by surface topography and physicochemical properties [13,14]. Collectively, these characteristics influence microbial adhesion and the biological behavior of restorative materials [15].

Surface finishing procedures are primary determinants of the surface integrity of feldspathic CAD/CAM ceramics [16,17]. However, daily toothbrushing may compromise the long-term stability of the surfaces produced by different finishing protocols [18]. Although glazing is traditionally considered the gold standard for achieving a smooth, homogeneous surface, the glaze layer may be partially or completely removed when intraoral occlusal or proximal adjustments are required, necessitating chairside polishing [6]. Polishing systems may yield different surface characteristics owing to differences in abrasive composition and application protocol [19]. Simulated toothbrushing is widely used to reproduce long-term clinical wear and to evaluate the durability of restorative materials [20,21]. Because wettability depends on both surface topography and physicochemical properties [13,14], toothbrushing may also alter wettability through mechanical abrasion and physicochemical surface changes.

Although the surface roughness of CAD/CAM ceramics has traditionally been assessed using two-dimensional parameters such as Ra (arithmetical mean roughness) [22], these measurements provide limited information about three-dimensional surface topography. Areal parameters, including Sa (arithmetical mean height), Sz (maximum height), Ssk (skewness), Sku (kurtosis), and Sdr (developed interfacial area ratio), provide complementary information on surface height, height distribution, and surface complexity [10,22]. Although previous studies have extensively investigated surface roughness, gloss, and color stability, fewer have examined wettability or the combined effects of finishing protocols and simulated toothbrushing. Evidence integrating these three-dimensional parameters

with wettability in feldspathic CAD/CAM ceramics, particularly following polishing before glazing, remains limited. This gap may be partly explained by the fact that most previous studies have assessed surface roughness using two-dimensional profile parameters such as Ra, which describe height variations along a single line only, and have rarely measured wettability together with surface topography. In addition, polishing before glazing has seldom been evaluated as a separate finishing protocol, since most studies have compared polished and glazed surfaces only with each other. Differences in measuring instruments, evaluation areas, and filtering procedures further complicate the comparison of areal roughness values among studies [10,23].

Therefore, the present study aimed to evaluate the effects of surface finishing protocols and simulated toothbrushing on three-dimensional surface topography (Sa, Sz, Ssk, Sku, and Sdr) and wettability of feldspathic CAD/CAM ceramics. In addition, surface morphology and elemental composition were examined descriptively on representative specimens using SEM and EDS. The null hypotheses were that (1) finishing protocols do not affect surface topography or wettability; (2) simulated toothbrushing does not affect these properties; and (3) there is no interaction between finishing protocol and toothbrushing for either outcome.

2. Materials and Methods

2.1. Study Design

This in vitro experimental study evaluated the effects of four different surface finishing protocols and simulated toothbrushing on the three-dimensional surface topography and wettability of feldspathic CAD/CAM ceramics.

2.2. Specimen Preparation

An a priori sample size calculation was performed using G*Power version 3.1.9.7 (Heinrich Heine University, Düsseldorf, Germany). The calculation was based on an F-test for a repeated-measures design with a within-between interaction, addressing the interaction between surface finishing protocol (four groups) and toothbrushing simulation (before and after toothbrushing). An effect size of f = 0.25, a significance level of $\alpha = 0.05$, a statistical power of 80%, a correlation among repeated measurements of 0.50, and a nonsphericity correction of 1.0 were assumed. Based on these parameters, a minimum total sample size of 48 specimens (12 per group) was required.

Forty-eight disc-shaped specimens measuring 10 mm in diameter and 1.2 mm in thickness were fabricated from feldspathic CAD/CAM ceramic blocks (CEREC Blocs, Dentsply Sirona, Bensheim, Germany) using a five-axis milling machine (Ceramill Motion 2, Amann Girrbach, Koblach, Austria).

To standardize the initial surfaces, all specimens were sequentially ground using a grinding machine (Phoenix Beta Grinder/Polisher; Buehler Ltd., Lake Bluff, IL, USA) with 320-, 400-, 600-, and 1200-grit silicon carbide papers at a constant speed of 300 rpm for 20 s under water cooling. Specimen thickness was verified using a digital caliper (Absolute Digimatic Caliper; Mitutoyo America Corporation, Aurora, IL, USA).

The specimens were subsequently cleaned in 99% alcohol for 3 min using an ultrasonic cleaner (Sonorex RK102 Transistor; BANDELIN electronic GmbH & Co. KG, Berlin, Germany). The specimens were then randomly allocated, using a computer-generated randomization sequence, to four experimental groups according to the surface finishing protocol applied:

1. OptraFine: polishing using a diamond-impregnated three-step ceramic polishing system (OptraFine; Ivoclar Vivadent, Schaan, Liechtenstein).

2. EVE: polishing using a diamond-impregnated three-step ceramic polishing system indicated for feldspathic ceramics (Diapol RA; EVE Ernst Vetter GmbH, Keltern, Germany).
3. Glaze: application of a ceramic glaze material (VITA AKZENT Plus GLAZE; VITA Zahnfabrik, Bad Säckingen, Germany).
4. OptraFine + Glaze: polishing with OptraFine followed by glaze application.

Polishing procedures were performed by a single calibrated operator using a low-speed contra-angle handpiece. The OptraFine Ceramic Polishing System and the Diapol RA Ceramic Polishing System were applied in their complete three-step sequences according to the manufacturers' instructions.

For the OptraFine group, the OptraFine F finisher (step 1) and the OptraFine P polisher (step 2) were used under continuous water cooling, followed by high-gloss polishing with the OptraFine HP nylon brush and diamond polishing paste (step 3) without water cooling, as recommended by the manufacturer. For the EVE group, the coarse (blue) smoothing polisher (step 1), the medium (pink) pre-polisher (step 2), and the fine (grey) high-gloss polisher (step 3) were used under continuous water cooling.

Each polishing step was performed for 30 s at 10,000 rpm, which is within the speed ranges recommended by the manufacturers, resulting in a total polishing time of 90 s per specimen, in accordance with previous studies on CAD/CAM ceramics [24–26]. A standardized manual force of approximately 2 N was applied with combined rotational and linear movements. The polishing instruments and nylon brushes were replaced after every five specimens to minimize the potential influence of instrument wear. After polishing, the specimens were ultrasonically cleaned to remove polishing residues and air-dried before the baseline measurements.

For the Glaze group, the glaze powder (VITA AKZENT Plus GLAZE; VITA Zahnfabrik, Bad Säckingen, Germany) was mixed with VITA AKZENT Plus POWDER FLUID according to the manufacturer's instructions to obtain a homogeneous consistency. The mixture was applied by the same operator with a fine brush as a single thin coat, using unidirectional strokes, to cover the entire specimen surface. Before firing, uniform coverage without pooling or uncovered areas was visually verified under a light source. The specimens were subsequently fired in a porcelain furnace (Programat P310; Ivoclar Vivadent, Schaan, Liechtenstein) according to the glaze manufacturer's recommended firing protocol for feldspathic CAD/CAM ceramics. The firing protocol included a pre-drying temperature of 500 °C, a pre-drying time of 4 min, a heating rate of 80 °C/min, a final firing temperature of 920 °C, and a holding time of 1 min without vacuum. After firing, the specimens were allowed to cool to room temperature under ambient laboratory conditions.

For the OptraFine + Glaze group, specimens were first polished using the standardized OptraFine protocol described above. Glaze was subsequently applied and fired using the same procedures as those described for the Glaze group.

2.3. Toothbrushing Simulation

Before simulated toothbrushing, the specimens were rinsed with distilled water. Each specimen was mounted in a multi-station toothbrushing simulator (DentArGe TB-6.1 Brushing Simulator; Analitik Medikal, Ankara, Türkiye). Brushing was performed at a frequency of 2 Hz and a brushing speed of 40 mm/s, using a linear reciprocating motion with a stroke length of 20 mm [27]. Each specimen was subjected to 20,000 brushing cycles, with one cycle defined as one complete back-and-forth movement. Because 10,000 brushing cycles have been reported to correspond to approximately 1 year of toothbrushing in the oral environment, 20,000 cycles were considered to simulate approximately 2 years of clinical toothbrushing [27,28].

A commercially available toothbrush head (CrossAction; Oral-B, Procter & Gamble, Cincinnati, OH, USA) was mounted perpendicular to the specimen surface in a custom-made stainless-steel holder, and a vertical load of 200 g (≈1.96 N) was applied throughout the simulation. In accordance with ISO 14569-1, a slurry was prepared by suspending 250 g of toothpaste (Colgate Total; Colgate-Palmolive, New York, NY, USA; relative dentin abrasivity ≈ 70) in 1 L of distilled water [29]. To maintain standardized abrasive conditions, the toothbrush head and slurry were replaced every 5000 cycles, corresponding to approximately 6 months of use, as previously described [30].

2.4. Surface Roughness Analysis

Three-dimensional surface roughness measurements were obtained before and after toothbrushing simulation using a non-contact optical profilometer (InfiniteFocus, Alicona Imaging GmbH, Graz, Austria).

Measurements were performed using a 20× objective over an evaluation area of 1250 × 1250 µm, with a vertical resolution of 50 nm and a lateral resolution of 0.9 µm. Following form removal, a Gaussian S-filter (λs) of 2.5 µm and an L-filter with a cut-off wavelength (λc) of 0.25 mm were applied in accordance with ISO 25178 prior to calculation of the areal parameters.

Quantitative surface characterization was performed using the ISO 25178 areal parameters [31] Sa (arithmetical mean height), Sz (maximum height), Ssk (skewness), Sku (kurtosis), and Sdr (developed interfacial area ratio). Three measurements were obtained from standardized regions of each specimen, and the mean value was used for statistical analysis.

2.5. Wettability Analysis

Surface wettability was evaluated by measuring the static water contact angle using a contact angle goniometer (Attension Theta Flex, Biolin Scientific, Espoo, Finland) using the sessile drop method.

Each specimen was positioned on the instrument stage, and a 5-µL droplet of distilled water was deposited on the surface using a micropipette. Droplet images were recorded using the integrated high-resolution camera and analyzed with the manufacturer's software. Measurements were performed under controlled ambient conditions at 23 ± 1 °C and a relative humidity of 50 ± 5%.

Contact angles were recorded as a function of time, and the value at 4 s after droplet deposition was used for statistical analysis to ensure measurement stability and reproducibility. Three measurements were performed for each specimen, and the mean value was used for statistical analysis. To estimate the contribution of surface topography to wettability, the Wenzel roughness ratio was approximated from the Sdr values ($r = 1 + Sdr/100$), and Young contact angles were calculated as $\cos \theta Y = \cos \theta^*/r$.

2.6. Scanning Electron Microscopy

Scanning electron microscopy (SEM) was performed to qualitatively evaluate surface morphology before and after toothbrushing simulation. Because gold sputter coating precludes further measurements on the same surface, two additional specimens per group ($n = 8$ in total) were prepared and finished as described in Section 2.2 and used exclusively for SEM; in each group, one specimen was examined before and the other after simulated toothbrushing performed as described in Section 2.3. The specimens were sputter-coated with gold and examined using a scanning electron microscope (ZEISS Sigma 300, Carl Zeiss AG, Oberkochen, Germany) at the East Anatolia High Technology Application and Research Center (DAYTAM), Atatürk University, Erzurum, Türkiye.

SEM images were obtained at a magnification of 500× using an accelerating voltage of 5.0 kV, a working distance of 5.1–6.9 mm, and an InLens secondary electron detector (Carl Zeiss AG, Oberkochen, Germany) under high vacuum. All images were acquired with identical settings before and after toothbrushing, and each micrograph covered an area of approximately 229 × 172 µm. For presentation, brightness and contrast were adjusted linearly and uniformly over each entire image, and no local or selective modifications were made. Characteristic surface features were marked with arrows and arrowheads. The micrographs were used for qualitative assessment of morphological differences associated with the applied surface finishing protocols and simulated toothbrushing.

2.7. Energy-Dispersive X-Ray Spectroscopy

The elemental composition of the specimen surfaces was evaluated semi-quantitatively by energy-dispersive X-ray spectroscopy (EDS) using an Octane Pro detector (EDAX, AMETEK Inc., Mahwah, NJ, USA) operated with TEAM software. For EDS analysis, one representative specimen was selected from each of the four experimental groups from among the 48 specimens used for quantitative surface measurements. EDS measurements were performed on the uncoated specimens before and after simulated toothbrushing. These specimens were distinct from the additional gold-coated specimens used for SEM examination.

Spectra were acquired from the full field of view at 500× magnification using an accelerating voltage of 20 kV, a take-off angle of approximately 33°, an amplifier time of 0.24 µs, and a live time of approximately 28 s. Quantification was performed using the standardless eZAF Smart Quant routine of the TEAM software (EDAX, AMETEK Inc., Mahwah, NJ, USA), and the results were expressed as weight and atomic percentages.

Elements detected close to the detection limit with relative errors exceeding 20%, or whose identification was ambiguous because of peak overlap, were excluded from the interpretation. Because the oxygen content is affected by matrix normalization, compositional changes were additionally evaluated using the atomic Na/Si and Al/Si ratios. As only one area per condition was analyzed, the EDS data were evaluated descriptively and were not subjected to statistical analysis.

2.8. Cross-Sectional SEM Analysis

To evaluate the glaze layer, one specimen from each glazed group (Glaze and OptraFine + Glaze) was examined before and after simulated toothbrushing. A notch approximately half the specimen thickness in depth was cut on the unglazed side of each specimen using a water-cooled diamond disc, and the specimen was fractured along the notch by manual bending. The fracture surfaces were examined without further polishing, as previously described [32]. After sputter-coating with gold, the cross-sections were examined using the same scanning electron microscope with an InLens secondary electron detector at an accelerating voltage of 5 kV and a magnification of 5000×. The continuity, relative thickness, and surface contour of the glaze layer were evaluated qualitatively, as only one specimen per condition was examined.

2.9. Statistical Analysis

Data were analyzed using IBM SPSS Statistics version 23.0 (IBM Corp., Armonk, NY, USA) and R software version 4.5.0 (R Foundation for Statistical Computing, Vienna, Austria). Descriptive statistics were calculated for all continuous variables and are presented as mean ± standard deviation.

The effects of surface finishing protocol, toothbrushing simulation, and the interaction between these factors on contact angle, Sa, Sz, Ssk, Sku, and Sdr values were evaluated using generalized estimating equations to account for the repeated measurements obtained

from the same specimens, and Wald chi-square statistics are reported where available. Bonferroni-adjusted pairwise comparisons were performed when significant main effects or interactions were identified. The significance level was set at $\alpha = 0.05$.

3. Results

3.1. Contact Angle

Surface finishing protocol, toothbrushing simulation, and their interaction significantly affected the contact angle (all $p < 0.001$; Table 1). Before toothbrushing, the polished groups (OptraFine and EVE) exhibited significantly higher contact angles than the glazed groups. After toothbrushing, contact angle decreased significantly in the OptraFine, EVE, and OptraFine + Glaze groups, whereas no significant change was observed in the Glaze group. The OptraFine + Glaze group exhibited the lowest contact angle at both time points, whereas no significant differences were found among the remaining groups after toothbrushing.

Table 1. Contact angle (°) values according to surface finishing protocol before and after 2-year toothbrushing simulation.

Group	Before Toothbrushing (°)	After Toothbrushing (°)	Overall Mean (°)
OptraFine	46.86 ± 5.65 ^{A}	26.72 ± 4.91 ^{B}	36.79 ± 11.62 ^{a}
EVE	49.49 ± 3.83 ^{A}	27.92 ± 3.99 ^{B}	38.71 ± 11.81 ^{a}
Glaze	26.82 ± 4.57 ^{B}	22.51 ± 6.29 ^{BC}	24.67 ± 5.73 ^{b}
OptraFine + Glaze	16.14 ± 2.48 ^{C}	12.28 ± 1.90 ^{D}	14.21 ± 2.92 ^{c}
Overall	34.83 ± 14.73	22.36 ± 7.60	—

Values are presented as mean ± standard deviation ($n = 12$ per group). Uppercase superscript letters (A–D) indicate comparisons among all group × time subgroups (interaction effect); subgroups sharing the same uppercase letter do not differ significantly. Lowercase superscript letters (a–c) indicate comparisons among the overall means of the finishing groups (main effect of finishing protocol); groups sharing the same lowercase letter do not differ significantly (Bonferroni-adjusted pairwise comparisons). Generalized estimating equation results: group, $p < 0.001$; time, $p < 0.001$; group × time, $p < 0.001$.

3.2. Surface Roughness

Sa was significantly affected by surface finishing protocol ($p < 0.001$) and by its interaction with toothbrushing simulation ($p = 0.007$), whereas the main effect of toothbrushing was not significant ($p = 0.185$) (Table 2). Before toothbrushing, the OptraFine group exhibited the lowest and the EVE group the highest Sa values, whereas the Glaze and OptraFine + Glaze groups did not differ significantly from each other. After toothbrushing, Sa increased significantly in the OptraFine and OptraFine + Glaze groups but did not change significantly in the Glaze and EVE groups. The OptraFine group remained significantly smoother than both glazed groups after toothbrushing, although it no longer differed significantly from the EVE group, and it exhibited the lowest Sa values irrespective of time.

Sz was significantly affected by surface finishing protocol ($p < 0.001$) and increased overall after toothbrushing ($p = 0.036$), without a significant interaction ($p = 0.615$); therefore, group-specific values are reported descriptively (Table 3). Irrespective of time, the OptraFine group exhibited significantly lower Sz values than the EVE and Glaze groups.

Table 2. Sa (μm) values according to surface finishing protocol before and after 2-year toothbrushing simulation.

Group	Before Toothbrushing (μm)	After Toothbrushing (μm)	Overall Mean (μm)
OptraFine	0.161 ± 0.061 ^{E}	0.194 ± 0.064 ^{D}	0.177 ± 0.062 ^{c}
EVE	0.376 ± 0.044 ^{A}	0.300 ± 0.067 ^{ABCD}	0.338 ± 0.074 ^{a}
Glaze	0.256 ± 0.030 ^{BCD}	0.310 ± 0.066 ^{ABC}	0.284 ± 0.056 ^{b}
OptraFine + Glaze	0.269 ± 0.056 ^{CD}	0.323 ± 0.079 ^{AB}	0.295 ± 0.072 ^{ab}
Overall	0.266 ± 0.090	0.282 ± 0.087	—

Values are presented as mean ± standard deviation (n = 12 per group). Uppercase superscript letters (A–E) indicate comparisons among all group × time subgroups (interaction effect); subgroups sharing the same uppercase letter do not differ significantly. Lowercase superscript letters (a–c) indicate comparisons among the overall means of the finishing groups (main effect of finishing protocol); groups sharing the same lowercase letter do not differ significantly (Bonferroni-adjusted pairwise comparisons). Generalized estimating equation results: group, Wald χ^2 = 39.265, $p < 0.001$; time, Wald χ^2 = 1.758, p = 0.185; group × time, Wald χ^2 = 12.058, p = 0.007. Sa, arithmetical mean height.

Table 3. Sz (μm) values according to surface finishing protocol before and after 2-year toothbrushing simulation.

Group	Before Toothbrushing (μm)	After Toothbrushing (μm)	Overall Mean (μm)
OptraFine	1.10 ± 0.29	1.67 ± 0.40	1.39 ± 0.45 ^{b}
EVE	2.14 ± 0.44	2.49 ± 0.58	2.32 ± 0.53 ^{a}
Glaze	2.06 ± 0.27	2.65 ± 0.92	2.35 ± 0.72 ^{a}
OptraFine + Glaze	1.99 ± 1.36	1.91 ± 0.59	1.95 ± 1.01 ^{ab}
Overall	1.82 ± 0.82	2.18 ± 0.74	—

Values are presented as mean ± standard deviation (n = 12 per group). Groups sharing a lowercase superscript letter do not differ significantly (Bonferroni-adjusted pairwise comparisons). Generalized estimating equation results: group, $p < 0.001$; time, p = 0.036; group × time, p = 0.615. Sz, maximum height.

3.3. Height Distribution and Hybrid Parameters

Ssk was negative in all groups at both time points, indicating valley-dominated surfaces (Table 4). Although surface finishing protocol had a significant overall effect on Ssk (p = 0.012), none of the pairwise comparisons was significant, and neither toothbrushing nor the interaction significantly affected Ssk. Sku was significantly affected by surface finishing protocol and toothbrushing (both $p \leq 0.010$), without a significant interaction, and the OptraFine + Glaze group exhibited significantly lower Sku values than all other groups. Sdr was significantly affected by surface finishing protocol ($p < 0.001$) and toothbrushing ($p < 0.001$), without a significant interaction; the OptraFine group exhibited the lowest Sdr values and differed significantly from the EVE and Glaze groups. Both Sku and Sdr increased overall after toothbrushing.

3.4. Surface Morphology

Representative SEM micrographs are presented in Figure 1. Before toothbrushing, the OptraFine surface appeared largely flat with scattered small, irregular features, whereas the EVE surface was more heterogeneous. The Glaze surface showed a vitreous appearance with prominent dendritic structures, whereas the OptraFine + Glaze surface appeared relatively homogeneous, with only sparse, small dendritic clusters. After toothbrushing, both polished surfaces exhibited small pits, accompanied by lamellar features in the OptraFine group and fine striations and irregular edges in the EVE group. The Glaze surface appeared largely

smooth, with shallow tracks and a continuous linear defect, and the dendritic structures were no longer evident. The OptraFine + Glaze surface showed alternating lighter and darker bands and fine scratches, the origin of which could not be determined from secondary electron images alone. As the micrographs before and after toothbrushing were obtained from different specimens, these observations were interpreted qualitatively.

Table 4. Ssk, Sku, and Sdr values according to surface finishing protocol before and after 2-year toothbrushing simulation.

Parameter/Group	Before Toothbrushing	After Toothbrushing	Overall Mean
Ssk			
OptraFine	−1.40 ± 0.32	−0.60 ± 0.79	−1.00 ± 0.71
EVE	−1.43 ± 0.10	−1.26 ± 0.87	−1.34 ± 0.60
Glaze	−0.92 ± 1.04	−0.76 ± 1.03	−0.84 ± 1.00
OptraFine + Glaze	−1.40 ± 0.25	−1.42 ± 0.13	−1.41 ± 0.19
Overall	−1.29 ± 0.57	−1.01 ± 0.81	—
Sku			
OptraFine	3.30 ± 0.27	3.56 ± 0.71	3.43 ± 0.53 [a]
EVE	2.92 ± 0.31	3.87 ± 1.42	3.39 ± 1.10 [a]
Glaze	2.88 ± 0.46	3.36 ± 0.38	3.12 ± 0.48 [a]
OptraFine + Glaze	2.58 ± 0.73	2.64 ± 0.46	2.61 ± 0.59 [b]
Overall	2.92 ± 0.52	3.36 ± 0.92	—
Sdr (%)			
OptraFine	0.81 ± 0.21	1.23 ± 0.29	1.02 ± 0.33 [a]
EVE	1.57 ± 0.33	1.82 ± 0.42	1.69 ± 0.39 [b]
Glaze	1.50 ± 0.20	1.94 ± 0.68	1.72 ± 0.53 [b]
OptraFine + Glaze	1.45 ± 1.00	1.40 ± 0.43	1.43 ± 0.74 [ab]
Overall	1.33 ± 0.60	1.60 ± 0.54	—

Values are presented as mean ± standard deviation (n = 12 per group). Within each parameter, lowercase superscript letters (a, b) indicate comparisons among the overall means of the finishing groups (main effect of finishing protocol); groups sharing a lowercase superscript letter do not differ significantly (Bonferroni-adjusted pairwise comparisons); for Ssk, no pairwise comparison was significant. Generalized estimating equation results: Ssk—group, $p = 0.012$; time, $p = 0.101$; group × time, $p = 0.074$. Sku—group, Wald $\chi^2 = 18.038$, $p < 0.001$; time, Wald $\chi^2 = 6.622$, $p = 0.010$; group × time, Wald $\chi^2 = 2.767$, $p = 0.429$. Sdr—group, Wald $\chi^2 = 53.836$, $p < 0.001$; time, Wald $\chi^2 = 12.835$, $p < 0.001$; group × time, Wald $\chi^2 = 6.356$, $p = 0.096$. Ssk, skewness; Sku, kurtosis; Sdr, developed interfacial area ratio.

3.5. Elemental Composition

The EDS results are summarized in Table 5, and representative spectra are presented in Figure 2. Before toothbrushing, the polished groups exhibited comparable compositions, consistent with the sodium–potassium aluminosilicate composition of the feldspathic ceramic (Al/Si atomic ratio, 0.47), whereas the glazed surfaces showed higher Na and lower Al and K contents (Al/Si, 0.16–0.18). After toothbrushing, the compositions of the polished surfaces changed only slightly, whereas both glazed groups shifted toward the composition of the ceramic substrate, with decreased Na and increased Al and K contents; the Al/Si ratio increased to 0.28 in the Glaze group and to 0.36 in the OptraFine + Glaze group. A small amount of Cl was detected on the OptraFine + Glaze surface, and no elements attributable to toothpaste constituents, such as F, P, Zn, or Sn, were detected on any surface.

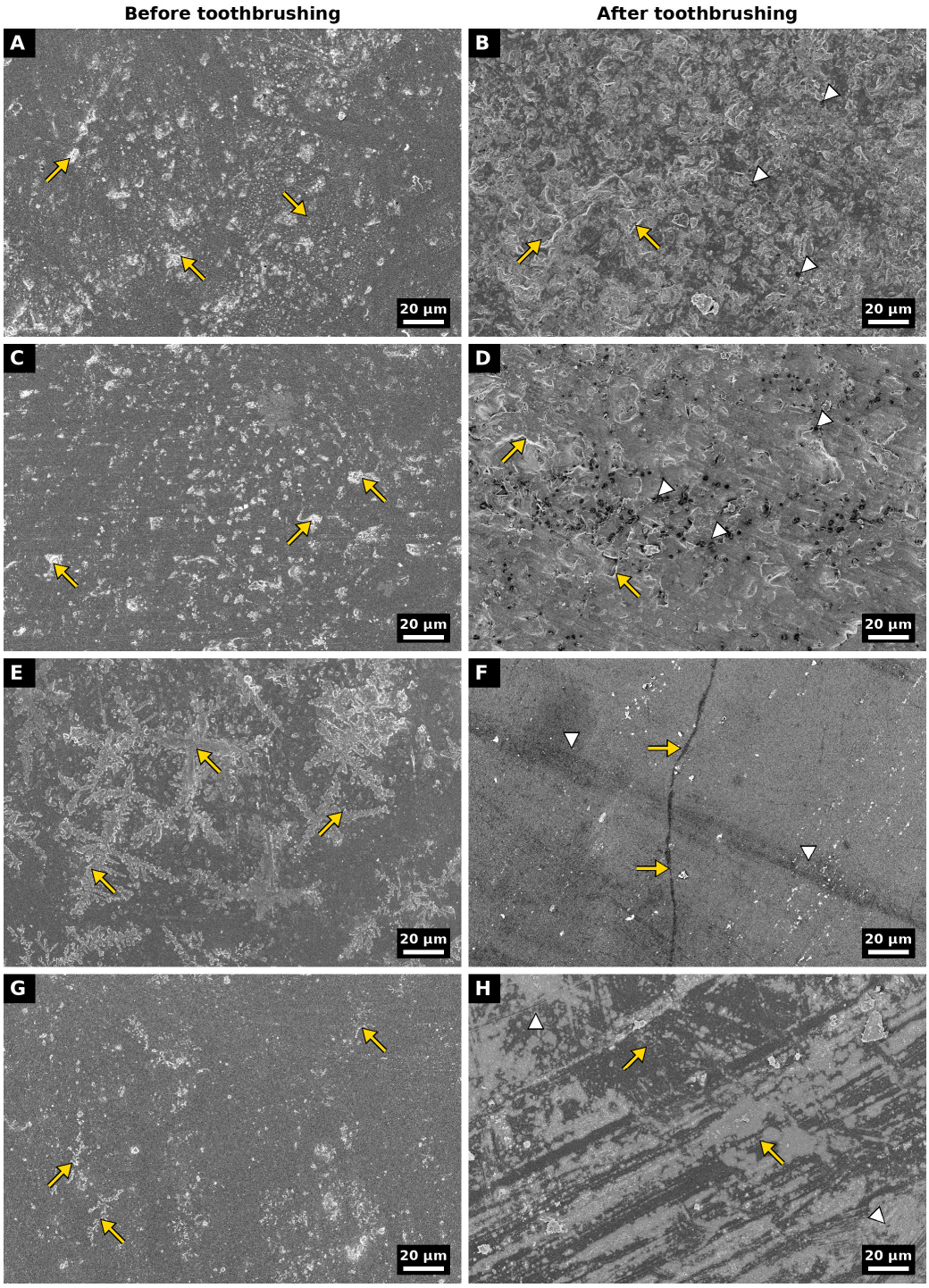


Figure 1. Representative scanning electron micrographs of feldspathic CAD/CAM ceramic surfaces before (left column) and after (right column) 2-year toothbrushing simulation. (**A**,**B**) OptraFine: (**A**) scattered irregular surface features (arrows); (**B**) lamellar features (arrows) and small pits (arrowheads). (**C**,**D**) EVE: (**C**) irregular surface features (arrows); (**D**) irregular edges (arrows) and small pits (arrowheads). (**E**,**F**) Glaze: (**E**) dendritic structures on the vitreous surface (arrows); (**F**) continuous linear defect (arrows) and shallow wear tracks (arrowheads). (**G**,**H**) OptraFine + Glaze: (**G**) sparse dendritic clusters (arrows); (**H**) lighter and darker bands oriented in the brushing direction (arrows), and fine scratches (arrowheads). All micrographs were obtained at 500× magnification with an accelerating voltage of 5.0 kV using an InLens detector. Scale bars = 20 µm.

Table 5. Elemental composition (wt%) and atomic Al/Si and Na/Si ratios of the specimen surfaces before (B) and after (A) 2-year toothbrushing simulation, determined by energy-dispersive X-ray spectroscopy.

Element	OptraFine		EVE		Glaze		OptraFine + Glaze	
	B	A	B	A	B	A	B	A
O	43.38	43.03	44.62	43.02	51.53	46.51	50.06	42.93
Na	8.88	8.32	9.04	8.55	17.34	13.40	17.34	11.79
Mg	—	—	—	—	1.25	—	0.86	—
Al	12.97	13.14	12.70	12.91	3.99	7.48	3.70	9.93
Si	29.01	29.95	28.20	29.54	22.78	27.39	23.72	28.63
K	5.76	5.56	5.07	5.99	2.37	3.91	2.20	4.49
Ca	—	—	—	—	0.75	1.32	0.82	1.40
Cl	—	—	—	—	—	—	0.29	0.83
Al/Si (at.)	0.47	0.46	0.47	0.46	0.18	0.28	0.16	0.36
Na/Si (at.)	0.37	0.34	0.39	0.35	0.93	0.60	0.89	0.50

Values are weight percentages obtained by standardless eZAF quantification from one representative area (500×, 20 kV) per condition; atomic ratios were calculated from atomic percentages. —, not detected. Elements detected close to the detection limit with relative errors > 20% (Ca, 0.38 wt%, EVE before toothbrushing; Ti, 0.30 wt%, OptraFine + Glaze before toothbrushing) and Mo (0.71 wt%, OptraFine + Glaze before toothbrushing), whose identification was ambiguous because of overlap of the Mo L and S K lines, are reported in this footnote only and were not included in the table or in the interpretation. B, before toothbrushing; A, after toothbrushing; at, atomic.

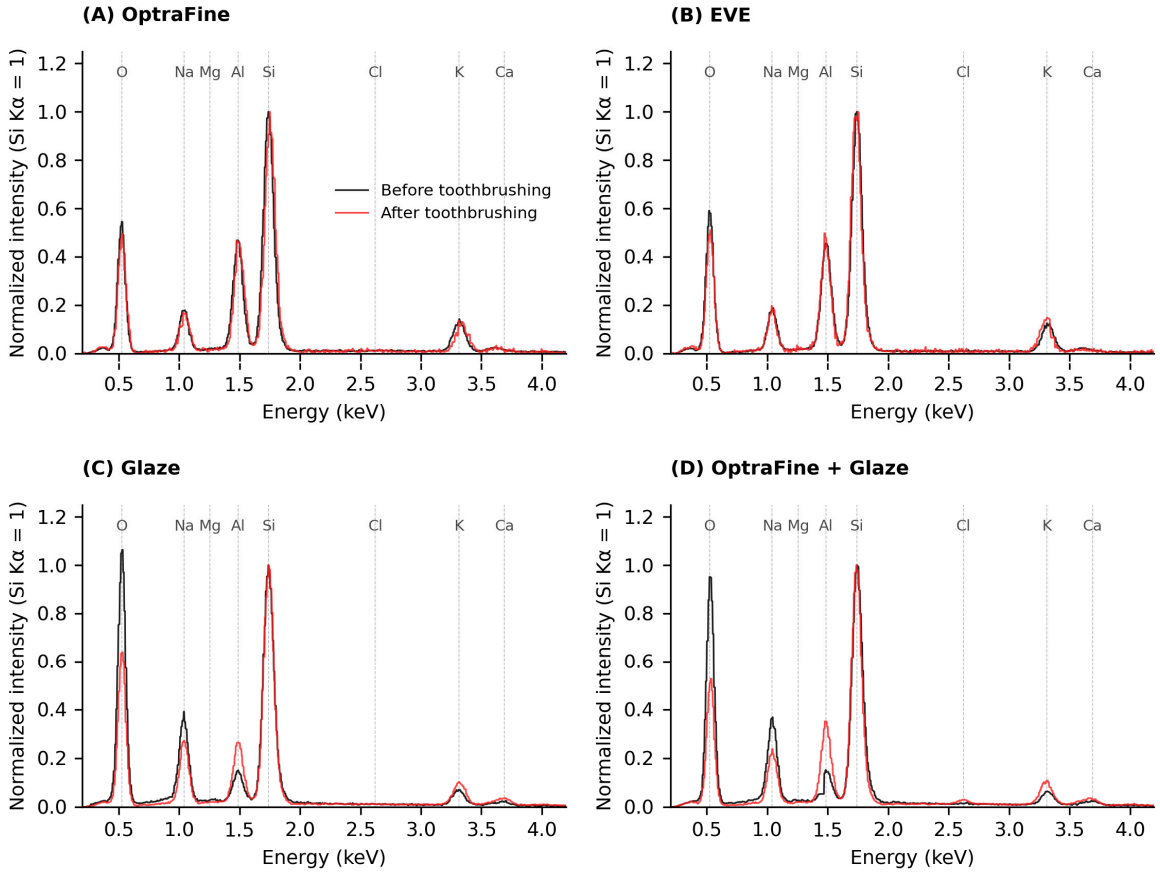


Figure 2. Representative energy-dispersive X-ray spectroscopy (EDS) spectra of feldspathic CAD/CAM ceramic surfaces before (black) and after (red) 2-year toothbrushing simulation: (**A**) OptraFine; (**B**) EVE; (**C**) Glaze; (**D**) OptraFine + Glaze. Spectra were acquired from the full field of view at 500× magnification and an accelerating voltage of 20 kV and were normalized to the

maximum intensity of the Si Kα peak to allow direct comparison of relative peak intensities. Dashed lines indicate the Kα energies of the labeled elements.

3.6. Cross-Sectional Morphology of the Glaze Layer

Representative cross-sectional SEM images of the glazed specimens are presented in Figure 3. Before toothbrushing, a continuous glaze layer that covered the ceramic surface and was morphologically distinguishable from the underlying ceramic was observed in both glazed groups. After toothbrushing, the glaze layer remained continuous in both groups but appeared thinner and more undulating than before toothbrushing.

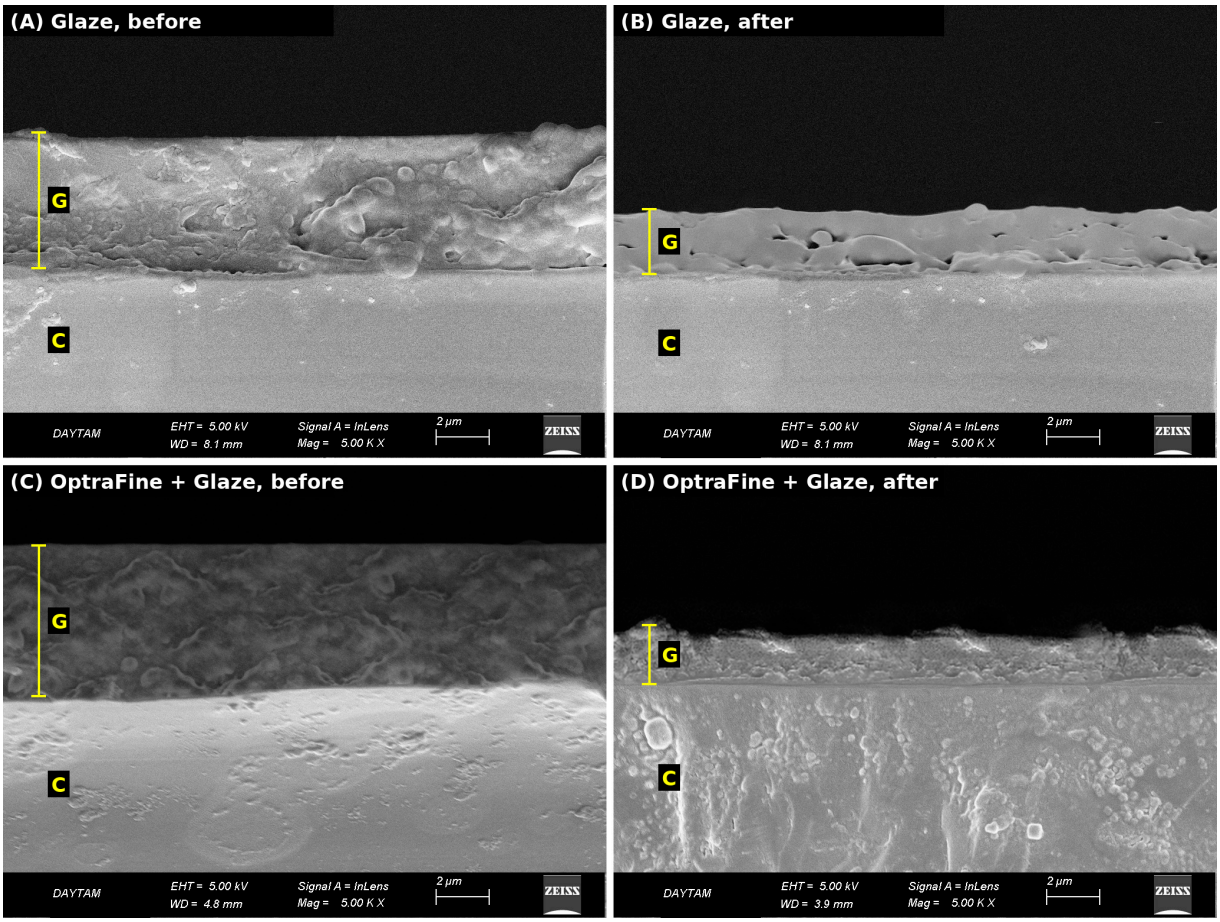


Figure 3. Representative cross-sectional SEM images of the glazed specimens (InLens detector, 5 kV, 5000×): (**A**) Glaze, before toothbrushing; (**B**) Glaze, after toothbrushing; (**C**) OptraFine + Glaze, before toothbrushing; (**D**) OptraFine + Glaze, after toothbrushing. G, glaze layer; C, feldspathic ceramic.

4. Discussion

This study demonstrated that the effects of simulated toothbrushing on the surface properties of feldspathic CAD/CAM ceramics depended on the surface finishing protocol, although this dependence was not consistent across all evaluated parameters. The first null hypothesis was rejected because the surface finishing protocols significantly affected all evaluated parameters. The second null hypothesis was partially rejected because simulated toothbrushing significantly decreased the contact angle and increased Sz, Sku, and Sdr values overall, whereas no significant overall main effect was found for Sa or Ssk. The third null hypothesis was also partially rejected because significant interactions between surface finishing protocol and toothbrushing were observed for Sa and contact angle, but not for Sz, Ssk, Sku, or Sdr.

To the best of our knowledge, no previous study has reported Sa values for feldspathic CAD/CAM ceramics under comparable measurement conditions. However, among studies on other glass–ceramics, Jurado et al. reported median Sa values of 0.32–0.34 µm for a chairside CAD/CAM lithium disilicate ceramic polished with ceramic polishing systems, including OptraFine [33]. The authors also noted that these values were below the surface roughness range of 0.45–0.65 µm reported for natural enamel [33,34]. Similarly, all finishing protocols applied to the feldspathic ceramic in the present study yielded mean Sa values of 0.161–0.376 µm before and 0.194–0.323 µm after toothbrushing, remaining below the range reported for enamel at both time points.

In the present study, the surfaces obtained by complete application of the OptraFine system exhibited the lowest roughness and remained smoother than both glazed surfaces after toothbrushing. This finding is consistent with the results of Gönüldaş et al. [35], who reported that polishing techniques produced smoother surfaces than glazing on feldspathic CAD/CAM ceramics, and of Carrabba et al. [24], who identified OptraFine, together with furnace glazing, among the systems that provided the lowest surface roughness. Hjerppe et al. [36], on the other hand, reported that glazed lithium disilicate surfaces exhibited lower Sa values than polished surfaces, but found no marked difference between glazed surfaces with and without prior polishing. The latter finding is consistent with the present results, whereas the former is not, suggesting that the effectiveness of surface finishing procedures may depend on the ceramic material, the polishing protocol, and the measurement approach.

Toothbrushing is the principal mechanical challenge to which restoration surfaces are exposed daily; therefore, the clinical benefit of a smooth surface achieved by finishing also depends on the extent to which it is preserved during brushing [18,20,21]. Although the effect of toothbrushing on feldspathic CAD/CAM ceramics has been evaluated in several studies [2,30,37,38], most of these studies relied on two-dimensional profile parameters such as Ra, and their findings are inconsistent; toothbrushing has been reported both to increase [30] and to decrease [37] the roughness of feldspathic ceramic. Because Ra may not reflect the local defects and changes in surface area produced by brushing, areal parameters such as Sz and Sdr are required to characterize these changes [10,22].

The significant interaction observed for Sa indicates that the response to brushing depended on the surface finishing protocol. The overall increases in Sz and Sdr, in turn, suggest that brushing created local defects and increased surface complexity rather than producing a uniform change in mean height. Çölgeçen and Barutçu attributed the roughening of feldspathic ceramic after brushing to the susceptibility of its brittle, glassy structure to microcrack formation under repeated frictional stress [30]; this mechanism may partly explain the present findings. The absence of a significant change in Sa in the Glaze group, however, differs from the findings of Vasiliu et al., who reported increased Ra and Rz values on glazed glass–ceramic surfaces after thermocycling [39,40]; differences in the aging method and measurement approach may have contributed to this discrepancy. SEM observations were largely consistent with the quantitative findings; the textured appearance of the OptraFine surface after brushing may reflect the fact that the two methods assessed different specimens at different scales.

Although the OptraFine and EVE systems have the same number of steps, they produced markedly different surfaces. Studies directly comparing these systems on glass–ceramics are limited and have reported partly inconsistent results. On CEREC Blocs, the same ceramic used in the present study, Wang et al. reported significantly lower Ra values with OptraFine than with an EVE system (DIAPRO) [41]. On VITABLOCS Mark II and IPS Empress CAD, Flury et al. found no difference in Ra but showed that OptraFine produced lower Rz values [25]. Alhabdan and El-Hejazi reported similar Ra values on a layered feldspathic veneering ceramic and a lithium disilicate ceramic, although fewer flaws were

observed by SEM on the OptraFine-polished surfaces [42]. The main difference between the two systems lies in the final step: OptraFine ends with a diamond polishing paste, whereas Diapol RA ends with a fine diamond-impregnated rubber polisher. Diamond pastes have been suggested to smooth the surface profile by rounding off the highest peaks [25], which may explain the lower Sz values of the OptraFine group. The discrepancies among studies may be attributed to differences in the ceramic material, the specific EVE product, and the measurement approach (two-dimensional profile versus three-dimensional areal parameters). To the best of our knowledge, no previous study has compared the behavior of feldspathic CAD/CAM ceramic surfaces polished with these two systems after toothbrushing. The fact that the difference between the two groups was no longer significant after brushing suggests that brushing may cause surfaces polished with different methods to converge toward a similar roughness level [37].

Consistent with this interpretation, Nima et al., who also measured Sa by non-contact laser microscopy, reported that the Sa of a feldspathic CAD/CAM ceramic (VITABLOCS Mark II) decreased after 30,000 brushing cycles and attributed this to the toothpaste abrasives acting as a prolonged polishing process that removed the highest surface peaks [37]. However, differences in experimental conditions, such as toothpaste abrasivity, number of cycles, and evaluation area, should be taken into account in this comparison.

The overall increases in Sku and Sz suggest an increased contribution of extreme values to the height distribution after brushing. The lower Sku values of the OptraFine + Glaze group indicate a height distribution with less pronounced peaks and valleys, suggesting that polishing before glazing may influence the height distribution even without changing the average roughness. Evaluating these parameters together enables the characterization of surface changes that conventional profile roughness measurements alone may not reveal [10,22].

Glazing may reduce surface irregularities by forming a vitreous surface layer; however, the long-term stability of this layer may be affected by mechanical wear [21,43]. The elemental composition of the polished surfaces was consistent with the sodium–potassium aluminosilicate structure reported for CEREC Blocs [5,44], and the absence of additional elements suggests that no detectable abrasive residues remained. The composition of the glazed surfaces, in contrast, supports the interpretation that glazing formed an alkali-rich vitreous layer distinct from the substrate.

The shift in the elemental composition of the glazed groups toward that of the feldspathic substrate after brushing is consistent with the cross-sectional SEM findings, in which the glaze layer appeared thinner and more undulating after brushing (Figure 3). Because the EDS signal at 20 kV may originate from a depth of several micrometers [45], a larger proportion of the signal may arise from the underlying ceramic as the glaze layer becomes thinner. However, alternative mechanisms, such as the brushing-induced removal of the dendritic structures of undetermined origin observed on the glazed surfaces before brushing, may also have contributed to the decrease in the Na/Si ratio. Findings consistent with glaze wear have also been reported previously: Barcellos et al. showed that the vitreous layer was removed after wear, exposing the underlying lithium disilicate [43], and Sulaiman et al. reported significant gloss loss after 30,000 brushing cycles on feldspathic ceramic coated with the same glaze system (VITA AKZENT Plus) and suggested that the glaze layer may be lost within the first months of clinical use [46].

SEM observations of the glazed groups also suggest that brushing modified the superficial characteristics of the glaze layer. Mahrous et al. [47] reported that brushing partially removed the superficial porous glaze layer of lithium disilicate ceramics, exposing the denser underlying glaze layer; the longer brushing period in the present study (approxi-

mately 2 years versus 1 year) may have contributed to the more pronounced changes in the glazed surfaces.

Toothbrushing increased wettability in all groups except the Glaze group, and this increase was accompanied by an overall increase in Sdr. According to the Wenzel model, an increase in the true surface area can enhance the wettability of hydrophilic surfaces ($\theta < 90°$) [13,14]. To estimate the magnitude of this contribution, the Wenzel roughness ratio was approximated from the measured Sdr values ($r = 1 + Sdr/100$), and the corresponding Young contact angles were calculated ($\cos \theta Y = \cos \theta^*/r$). Because the Sdr values ranged from 0.81% to 1.94%, the calculated r values were close to unity (1.008–1.019), and the Young contact angles differed from the measured contact angles by approximately 3° or less in all groups; this difference is small compared with the change in contact angle observed after brushing. Therefore, the topographic changes detectable by profilometry can account for only a minor part of the change in wettability (Figure 4). Moreover, the absence of a significant interaction for Sdr despite the group-dependent change in contact angle and the largely unchanged EDS composition of the polished groups despite the marked decrease in their contact angle suggest that changes in wettability cannot be explained by topography or elemental composition alone [5,14]. Brushing-induced physicochemical surface changes may also have contributed to the increase in wettability [48–51]. Although wettability may influence pellicle formation [52], microbial adhesion is affected by numerous factors, including surface roughness and topography, surface free energy and hydrophobicity, surface chemistry and charge, the composition of the acquired pellicle, the characteristics of the bacterial species (e.g., cell-surface hydrophobicity, adhesins, and motility), and the hydrodynamic conditions in the oral cavity [7,15,53]; therefore, increased wettability should not be interpreted as direct evidence of increased or decreased biofilm formation [10,53].

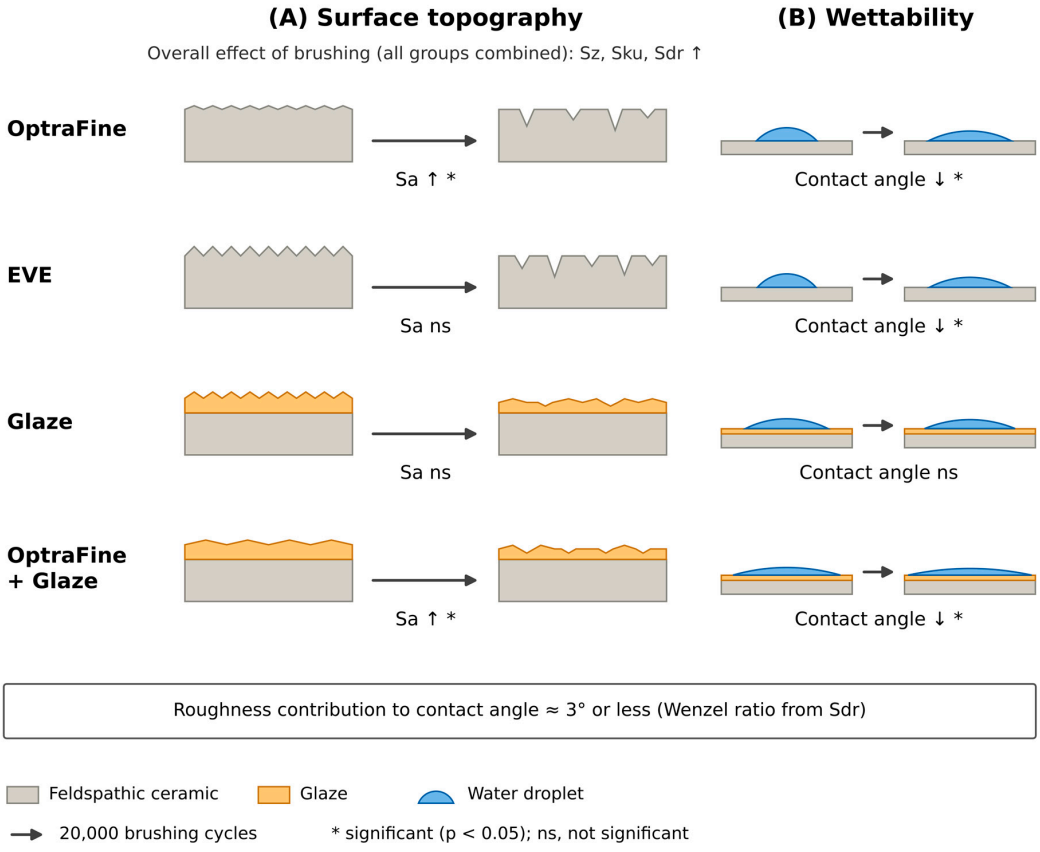


Figure 4. Schematic illustration of the changes in (**A**) surface topography and (**B**) wettability of the four finishing groups after 20,000 cycles of simulated toothbrushing. Significance symbols refer to

the Bonferroni-adjusted pairwise comparisons between before and after toothbrushing within each group (Tables 1 and 2): *, significant difference ($p < 0.05$); ns, not significant. Changes in Sz, Sku, and Sdr represent overall main effects of toothbrushing, without significant interaction with the finishing protocol. Droplet shapes correspond to the mean measured contact angles. Features are not drawn to scale.

4.1. Clinical Implications

Within the limitations of this study, when intraoral adjustment of a glazed feldspathic CAD/CAM restoration is required, chairside polishing with a multistep diamond polishing system such as OptraFine may be performed instead of removing the restoration for reglazing. However, because polishing systems with the same number of steps may not provide equivalent results, clinicians are advised to follow the complete sequence recommended by the manufacturer, including the final step with diamond paste. For restorations glazed in the laboratory before delivery, polishing before glazing did not reduce the average roughness but resulted in a height distribution with less pronounced peaks and valleys; the clinical relevance of this difference should be evaluated in future studies. Because glazed surfaces may also undergo brushing-induced changes, periodic clinical follow-up of these restorations is recommended. Because bacterial adhesion and other biological parameters were not evaluated, these recommendations are based on surface characteristics only and should be confirmed by further in vitro and clinical studies.

4.2. Limitations

This study has several limitations. The in vitro design, the use of a single ceramic, and a single brushing regimen that did not include factors such as thermal changes, masticatory loading, and acidic challenges limit the generalizability of the findings to clinical conditions. Optical profilometry of translucent glass–ceramic surfaces may be affected by measurement noise, particularly for Sz. SEM, EDS, and cross-sectional evaluations were each limited to a single, separate specimen per condition and were therefore interpreted qualitatively. Glaze layer thickness was not quantified, and surface free energy was not determined; therefore, the proposed mechanisms underlying the compositional changes in the glazed surfaces and the increase in wettability should be regarded as tentative. Dynamic (advancing and receding) contact angles were not measured, and surface contamination was not quantified. In addition to addressing these limitations, future studies should include other glass–ceramics and polishing systems, evaluate gloss as a clinically relevant esthetic parameter, and examine the biological relevance of the observed changes together with pellicle formation and bacterial adhesion.

5. Conclusions

Within the limitations of this in vitro study, the following conclusions can be drawn:

1. The surface finishing protocol affected the three-dimensional surface topography and wettability of the feldspathic CAD/CAM ceramic. The complete three-step OptraFine sequence produced the lowest average surface roughness (Sa) and remained smoother than both glazed groups after simulated toothbrushing corresponding to approximately 2 years of clinical use.
2. The effect of toothbrushing on Sa depended on the finishing protocol: Sa increased significantly in the OptraFine and OptraFine + Glaze groups but not in the EVE and Glaze groups. In contrast, toothbrushing increased Sz, Sku, and Sdr overall, without a significant interaction with the finishing protocol, suggesting the formation of local surface defects rather than a uniform change in mean height.
3. Toothbrushing decreased the water contact angle in all groups except the Glaze group.

4. Polishing before glazing did not reduce Sa compared with glazing alone but resulted in the lowest Sku values and the lowest contact angle.

Two diamond polishing systems with the same number of steps produced markedly different surfaces; therefore, these findings should not be generalized to other polishing systems or ceramic materials.

Author Contributions: Conceptualization, Z.Y. and F.S.; methodology, Z.Y., Z.A. and F.S.; validation, Z.Y. and F.S.; formal analysis, Z.A. and F.S.; investigation, Z.A.; data curation, Z.A.; writing—original draft preparation, Z.A.; writing—review and editing, Z.Y., Z.A. and F.S.; visualization, Z.A.; supervision, Z.Y. All authors have read and agreed to the published version of the manuscript.

Funding: This research received no external funding.

Institutional Review Board Statement: This study did not involve human participants, human data, human tissue, or animals. Ethical approval was therefore not required.

Informed Consent Statement: Not applicable.

Data Availability Statement: The data that support the findings of this study are available from the corresponding author upon reasonable request.

Conflicts of Interest: The authors declare no conflicts of interest.

References

1. Suganna, M.; Kausher, H.; Ahmed, S.T.; Alharbi, H.S.; Alsubaie, B.F.; Ds, A.; Haleem, S.; Ali, A.B.M.R. Contemporary evidence of CAD-CAM in dentistry: A systematic review. *Cureus* **2022**, *14*, e31687. [CrossRef]
2. Yuan, J.C.-C.; Barão, V.A.R.; Wee, A.G.; Alfaro, M.F.; Afshari, F.S.; Sukotjo, C. Effect of brushing and thermocycling on the shade and surface roughness of CAD-CAM ceramic restorations. *J. Prosthet. Dent.* **2018**, *119*, 1000–1006. [CrossRef]
3. Montazerian, M.; Zanotto, E.D. Bioactive and inert dental glass-ceramics. *J. Biomed. Mater. Res. A* **2017**, *105*, 619–639. [CrossRef]
4. Kruzic, J.J.; Arsecularatne, J.A.; Tanaka, C.B.; Hoffman, M.J.; Cesar, P.F. Recent advances in understanding the fatigue and wear behavior of dental composites and ceramics. *J. Mech. Behav. Biomed. Mater.* **2018**, *88*, 504–533. [CrossRef]
5. Boanca, C.; Earar, K.; Focsaneanu, S.C.; Cocoș, D.I.; Budacu, C.C. Evaluation of the surface properties of three CAD/CAM ceramics: A comparative in vitro study. *Dent. J.* **2025**, *13*, 550. [CrossRef]
6. Hmaidouch, R.; Müller, W.-D.; Lauer, H.-C.; Weigl, P. Surface roughness of zirconia for full-contour crowns after clinically simulated grinding and polishing. *Int. J. Oral Sci.* **2014**, *6*, 241–246. [CrossRef]
7. Zheng, S.; Bawazir, M.; Dhall, A.; Kim, H.-E.; He, L.; Heo, J.; Hwang, G. Implication of surface properties, bacterial motility, and hydrodynamic conditions on bacterial surface sensing and their initial adhesion. *Front. Bioeng. Biotechnol.* **2021**, *9*, 643722. [CrossRef]
8. Zissis, A.J.; Polyzois, G.L.; Yannikakis, S.A.; Harrison, A. Roughness of denture materials: A comparative study. *Int. J. Prosthodont.* **2000**, *13*, 136–140.
9. Bollen, C.M.L.; Lambrechts, P.; Quirynen, M. Comparison of surface roughness of oral hard materials to the threshold surface roughness for bacterial plaque retention: A review of the literature. *Dent. Mater.* **1997**, *13*, 258–269. [CrossRef]
10. Schubert, A.; Wassmann, T.; Holtappels, M.; Kurbad, O.; Krohn, S.; Bürgers, R. Predictability of microbial adhesion to dental materials by roughness parameters. *Coatings* **2019**, *9*, 456. [CrossRef]
11. Gittens, R.A.; Scheideler, L.; Rupp, F.; Hyzy, S.L.; Geis-Gerstorfer, J.; Schwartz, Z.; Boyan, B.D. A review on the wettability of dental implant surfaces II: Biological and clinical aspects. *Acta Biomater.* **2014**, *10*, 2907–2918. [CrossRef]
12. Yulianto, H.D.K.; Rinastiti, M. Contact angle measurement of dental restorative materials by drop profile image analysis. *J. Teknosains* **2014**, *3*, 112–119. [CrossRef]
13. Rupp, F.; Gittens, R.A.; Scheideler, L.; Marmur, A.; Boyan, B.D.; Schwartz, Z.; Geis-Gerstorfer, J. A review on the wettability of dental implant surfaces I: Theoretical and experimental aspects. *Acta Biomater.* **2014**, *10*, 2894–2906. [CrossRef]
14. Noro, A.; Kaneko, M.; Murata, I.; Yoshinari, M. Influence of surface topography and surface physicochemistry on wettability of zirconia (tetragonal zirconia polycrystal). *J. Biomed. Mater. Res. B Appl. Biomater.* **2013**, *101*, 355–363. [CrossRef]
15. Song, F.; Koo, H.; Ren, D. Effects of material properties on bacterial adhesion and biofilm formation. *J. Dent. Res.* **2015**, *94*, 1027–1034. [CrossRef]
16. Fraga, S.; Amaral, M.; Bottino, M.A.; Valandro, L.F.; Kleverlaan, C.J.; May, L.G. Impact of machining on the flexural fatigue strength of glass and polycrystalline CAD/CAM ceramics. *Dent. Mater.* **2017**, *33*, 1286–1297. [CrossRef]

17. Etöz, O.; Tanrıkut, Ö.O.; Karadeniz, N.; Kavut, İ.; Yapıcı Gülbey, D.E. Effects of surface finishing procedures on the color, gloss, and surface roughness of CAD/CAM ceramics after coffee aging: An in vitro study. *Anatol. Curr. Med. J.* **2026**, *8*, 159–166. [CrossRef]
18. Geduk, Ş.E.; Sağlam, G. The effect of whitening toothpastes on the surface properties and color stability of different ceramic materials. *BMC Oral Health* **2024**, *24*, 1305. [CrossRef]
19. Tholt, B.; Miranda-Júnior, W.G.; Prioli, R.; Thompson, J.; Oda, M. Surface roughness in ceramics with different finishing techniques using atomic force microscope and profilometer. *Oper. Dent.* **2006**, *31*, 442–449. [CrossRef]
20. Bataweel, O.O.; Roulet, J.F.; Rocha, M.G.; Zoidis, P.; Pereira, P.; Delgado, A.J. Effect of simulated tooth brushing on surface roughness, gloss, and color stability of milled and printed permanent restorative materials. *J. Esthet. Restor. Dent.* **2025**, *37*, 1773–1783. [CrossRef]
21. Garza, L.A.; Thompson, G.; Cho, S.-H.; Berzins, D.W. Effect of toothbrushing on shade and surface roughness of extrinsically stained pressable ceramics. *J. Prosthet. Dent.* **2016**, *115*, 489–494. [CrossRef]
22. Sampaio-Fernandes, M.; Almeida, P.J.; Almeida, P.R.; Portugal, J.; Martins, R.C.; Figueiral, M.H. Effectiveness of ceramics chair-side polishing—2D and 3D roughness evaluation. *Rev. Port. Estomatol. Med. Dent. Cir. Maxilofac.* **2022**, *63*, 126–133. [CrossRef]
23. Mory, N.; Cascos, R.; Celemín-Viñuela, A.; Gómez-Polo, C.; Agustín-Panadero, R.; Gómez-Polo, M. Comparison of the surface roughness of CAD/CAM metal-free materials used for complete-arch implant-supported prostheses: An in vitro study. *Biomedicines* **2023**, *11*, 3036. [CrossRef]
24. Carrabba, M.; Vichi, A.; Vultaggio, G.; Pallari, S.; Paravina, R.; Ferrari, M. Effect of finishing and polishing on the surface roughness and gloss of feldspathic ceramic for chairside CAD/CAM systems. *Oper. Dent.* **2017**, *42*, 175–184. [CrossRef]
25. Flury, S.; Lussi, A.; Zimmerli, B. Performance of different polishing techniques for direct CAD/CAM ceramic restorations. *Oper. Dent.* **2010**, *35*, 470–481. [CrossRef]
26. Alrabiah, M.; Binrayes, A.; Alsayed, H.D.; Althumairy, R.I.; Habib, S.R. Chairside finishing and polishing of modern dental ceramics: Material-specific variations in surface roughness. *Front. Mater.* **2026**, *12*, 1744731. [CrossRef]
27. Kaynak Öztürk, E.; Binici Aygün, E.; Çiçek, E.S.; Sağlam, G.; Turhan Bal, B.; Karakoca Nemli, S.; Bankoğlu Güngör, M. Effects of surface finishing procedures, coffee immersion, and simulated tooth-brushing on the surface roughness, surface gloss, and color stability of a resin matrix ceramic. *Coatings* **2025**, *15*, 627. [CrossRef]
28. Prasad, M.; Rajula, P.B.; Pl, R.; Rao, S.; Gayathri, K.; Mounika, V.; Kodali, M.V.R.M.; Kalaivani, V.; Soloman, G.; Nisha, N. In vitro analysis of enamel abrasion using a novel manual nano-bristle toothbrush: An atomic force microscopy study. *Cureus* **2024**, *16*, e75243. [CrossRef]
29. *ISO 14569-1:2007*; Dental Materials—Guidance on Testing of Wear—Part 1: Wear by Tooth Brushing. International Organization for Standardization: Geneva, Switzerland, 2007.
30. Çölgeçen, Ö.; Barutçu, A.C. Surface degradation and digital volumetric loss in ceramic and hybrid CAD/CAM surfaces after simulated toothbrushing with activated charcoal vs. whitening toothpaste. *BMC Oral Health* **2026**, *26*, 208. [CrossRef]
31. *ISO 25178-2:2021*; Geometrical Product Specifications (GPS)—Surface Texture: Areal—Part 2: Terms, Definitions and Surface Texture Parameters. International Organization for Standardization: Geneva, Switzerland, 2021.
32. Nonaka, K.; Teramae, M.; Pezzotti, G. Mechanisms of Strength Degradation of Dental Zirconia Due to Glazing: Dependence on Glaze Thickness. *Materials* **2025**, *18*, 684. [CrossRef]
33. Jurado, C.A.; Amarillas-Gastelum, C.; Afrashtehfar, K.I.; Argueta-Figueroa, L.; Fischer, N.G.; Alshabib, A. Ceramic and composite polishing systems for milled lithium disilicate restorative materials: A 2D and 3D comparative in vitro study. *Materials* **2022**, *15*, 5402. [CrossRef]
34. Mullan, F.; Austin, R.S.; Parkinson, C.R.; Hasan, A.; Bartlett, D.W. Measurement of surface roughness changes of unpolished and polished enamel following erosion. *PLoS ONE* **2017**, *12*, e0182406. [CrossRef]
35. Gönüldaş, F.; Öztürk, C.; Atalay, P.; Öztaş, D. Influence of different surface finishing techniques on machinable feldspathic and leucite-reinforced ceramics. *Dent. Mater. J.* **2019**, *38*, 317–322. [CrossRef]
36. Hjerppe, J.; Shahramian, K.; Rosqvist, E.; Lassila, L.V.J.; Peltonen, J.; Närhi, T.O. Gastric acid challenge of lithium disilicate-reinforced glass–ceramics and zirconia-reinforced lithium silicate glass–ceramic after polishing and glazing—Impact on surface properties. *Clin. Oral Investig.* **2023**, *27*, 6865–6877. [CrossRef]
37. Nima, G.; Lugo-Varillas, J.; Soto, J.; Faraoni, J.; Palma-Dibb, R.; Correa-Medina, A.; Giannini, M. Effect of tooth brushing on the surface of enamel and direct and indirect CAD/CAM restorative materials. *Int. J. Prosthodont.* **2021**, *34*, 473–481. [CrossRef]
38. Flury, S.; Diebold, E.; Peutzfeldt, A.; Lussi, A. Effect of artificial toothbrushing and water storage on the surface roughness and micromechanical properties of tooth-colored CAD-CAM materials. *J. Prosthet. Dent.* **2017**, *117*, 767–774. [CrossRef]
39. Vasiliu, R.-D.; Porojan, S.D.; Bîrdeanu, M.I.; Porojan, L. Effect of thermocycling, surface treatments and microstructure on the optical properties and roughness of CAD-CAM and heat-pressed glass ceramics. *Materials* **2020**, *13*, 381. [CrossRef]
40. Vasiliu, R.-D.; Porojan, S.-D.; Bîrdeanu, M.-I.; Uțu, I.-D.; Porojan, L. The effect of thermocycling and surface treatments on the surface roughness and microhardness of three heat-pressed ceramics systems. *Crystals* **2020**, *10*, 160. [CrossRef]

41. Wang, T.; Guo, Z.; Guo, H.; Qiao, X. Polishing performance of different polishing tools for CEREC Blocs ceramic. *Hua Xi Kou Qiang Yi Xue Za Zhi* **2017**, *35*, 171–175. (In Chinese) [CrossRef]
42. Alhabdan, A.A.; El-Hejazi, A.A. Comparison of surface roughness of ceramics after polishing with different intraoral polishing systems using profilometer and SEM. *J. Dent. Health Oral Disord. Ther.* **2015**, *2*, 101–111. [CrossRef]
43. Barcellos, A.S.P.; Miranda, J.S.; Amaral, M.; Alvarenga, J.A.; Nogueira, L.; Kimpara, E.T. Effect of staining on the mechanical, surface and biological properties of lithium disilicate. *Saudi Dent. J.* **2022**, *34*, 136–141. [CrossRef]
44. AlShehri, K.A.A.; Rayyan, M.R. Effect of simulated tooth brushing on the surface gloss of monolithic all-ceramic restorations: An in vitro study. *Clin. Oral Investig.* **2025**, *29*, 133. [CrossRef]
45. Kanaya, K.; Okayama, S. Penetration and energy-loss theory of electrons in solid targets. *J. Phys. D Appl. Phys.* **1972**, *5*, 43–58. [CrossRef]
46. Sulaiman, T.A.; Camino, R.N.; Cook, R.; Delgado, A.J.; Roulet, J.-F.; Clark, W.A. Time-lasting ceramic stains and glaze: A toothbrush simulation study. *J. Esthet. Restor. Dent.* **2020**, *32*, 581–585. [CrossRef]
47. Mahrous, A.A.; Alhammad, A.; Alqahtani, F.; Aljar, Y.; Alkadi, A.; Taymour, N.; Alotaibi, A.; Akhtar, S.; Gad, M.M. The toothbrushing effects on surface properties and color stability of CAD/CAM and pressable ceramic fixed restorations—An in vitro study. *Materials* **2023**, *16*, 2950. [CrossRef]
48. Preston, D.J.; Miljkovic, N.; Sack, J.; Enright, R.; Queeney, J.; Wang, E.N. Effect of hydrocarbon adsorption on the wettability of rare earth oxide ceramics. *Appl. Phys. Lett.* **2014**, *105*, 011601. [CrossRef]
49. Watanabe, H.; Saito, K.; Kokubun, K.; Sasaki, H.; Yoshinari, M. Change in surface properties of zirconia and initial attachment of osteoblastlike cells with hydrophilic treatment. *Dent. Mater. J.* **2012**, *31*, 806–814. [CrossRef]
50. Esquivel-Upshaw, J.F.; Dieng, F.Y.; Clark, A.E.; Neal, D.; Anusavice, K.J. Surface degradation of dental ceramics as a function of environmental pH. *J. Dent. Res.* **2013**, *92*, 467–471. [CrossRef]
51. Kang, S.U.; Lee, D.-Y.; Kim, Y.-K.; Kim, S.-J.; Kim, H.-K.; Kim, C.-H. Effect of various storage media on the physicochemical properties of plasma-treated dental zirconia. *Sci. Rep.* **2024**, *14*, 25895. [CrossRef]
52. Sterzenbach, T.; Helbig, R.; Hannig, C.; Hannig, M. Bioadhesion in the oral cavity and approaches for biofilm management by surface modifications. *Clin. Oral Investig.* **2020**, *24*, 4237–4260. [CrossRef]
53. Katsikogianni, M.; Missirlis, Y.F. Concise review of mechanisms of bacterial adhesion to biomaterials and of techniques used in estimating bacteria-material interactions. *Eur. Cells Mater.* **2004**, *8*, 37–57. [CrossRef]

Disclaimer/Publisher's Note: The statements, opinions and data contained in all publications are solely those of the individual author(s) and contributor(s) and not of MDPI and/or the editor(s). MDPI and/or the editor(s) disclaim responsibility for any injury to people or property resulting from any ideas, methods, instructions or products referred to in the content.